

Supporting Information

Role of Molecular Symmetry on the Magnetic Relaxation Dynamics of Five-Coordinate Dy(III) Complexes

Yan Guo^{†a,b}, Kang Liu^{†,a}, Yuanyuan Qin^{†,b}, Qun-Yan Wu^a, Kong-Qiu Hu^a, Lei Mei^a,
Zhi-Fang Chai,^a Xiang-Yu Liu^{*,b}, Ji-Pan Yu^{*,a} and Wei-Qun Shi^{*,a}

^aLaboratory of Nuclear Energy Chemistry, Institute of High Energy Physics, Chinese Academy of Sciences, Beijing, 100049, China

^bState Key Laboratory of High-efficiency Utilization of Coal and Green Chemical Engineering, College of Chemistry and Chemical Engineering, Ningxia University, Yinchuan 750021, China.

Table of Contents

Table S1 Selected crystallographic data and structure refinement for complexes 1-3	3
Table S2 Selected Bond Lengths (Å) and Bond Angles (°) for 1-3	4
Table S3 Relaxation fitting parameters from least-squares fitting of $\chi(f)$ data under 500 Oe dc field of 1	6
Table S4 Relaxation fitting parameters from least-squares fitting of $\chi(f)$ data under 500 Oe dc field of 2	6
Table S5 Relaxation fitting parameters from least-squares fitting of $\chi(f)$ data under 500 Oe dc field of 3	6
Table S6 Calculated energy levels (cm^{-1}), g (g_x, g_y, g_z) tensors and predominant m_J values of the lowest eight Kramers doublets (KDs) of complexes 1a, 1b, 2 and 3 , using CASSCF/RASSI-SO with OpenMolcas.....	7
Table S7 Wave functions with definite projection of the total moment $ m_J\rangle$ for the lowest eight KDs of complexes 1a, 1b, 2 and 3 using CASSCF/RASSI-SO with OpenMolcas.....	8
Table S8 Calculated crystal-field parameters $B(k, q)$ and the corresponding weights for compounds 1a, 1b, 2 and 3 using CASSCF/RASSI-SO with OpenMolcas.	9
Table S9 Continuous Shape Measures (<i>CShM</i>) calculations for complexes 1-3	10
Table S10 Crystal field parameters for 1-3 fitted from magnetic data.....	11
Table S11 Energy levels and g for 1-3 fitted from magnetic data.....	11
Fig. S1 Packing arrangement of 1 along the crystallographic b axis.	11
Fig. S2 Packing arrangement of 2 along the crystallographic a axis.	12
Fig. S3 Packing arrangement of 3 along the crystallographic a axis.	12
Fig. S4 PXRD patterns for complex 1	13
Fig. S5 PXRD patterns for complex 2	13
Fig. S6 PXRD patterns for complex 3	14
Fig. S7 Plots of M vs. H/T for 1-3 at different temperature.	14
Fig. S8 Temperature dependence of the in-phase (top) and out (bottom) ac susceptibilities at different frequencies without a dc field for complexes 1-3	14
Fig. S9 Frequency dependence of the in-phase (top) and out (bottom) ac susceptibilities at different frequencies without a dc field for complexes 1-3	15
Fig. S10 Temperature dependence of the in-phase (top) and out-of-phase (bottom) ac susceptibilities at different frequencies with a dc field of 500 Oe for complexes 1 (a, a'), 2 (b, b') and 3 (c, c'). ...	15
Fig. S11 Temperature dependent relaxation times of 1 (a), 2 (b) and 3 (c) (log-log scale) under a 500Oe dc field. The lines were fitted to the equation of $\tau = T^{-n}$ to give n values.	16
Fig. S12 Calculated molecular structures of complexes 1a (a), 1b (b), 2 (c) and 3 (d); H atoms are omitted for clarify.	16
Fig. S13 Magnetization relaxation time, $\ln \tau$ vs. T^{-1} plot under 500Oe dc field for 1 (a), 3 (b). The green line represents the Arrhenius fit.	17
References	17

Table S1 Selected crystallographic data and structure refinement for complexes **1-3**.

Identification code	1	2	3
Empirical formula	C ₆₈ H ₁₀₆ Dy ₂ N ₈ O ₂ Si ₆	C ₃₅ H ₅₀ DyN ₅ Si ₃	C ₃₃ H ₅₄ DyN ₅ OSi ₃
Formula weight	1561.14	787.57	783.58
Temperature/K	150.0	170	170
Wavelength/Å	0.71073	1.54178	0.71073
Crystal system	monoclinic	monoclinic	monoclinic
Space group	<i>P</i> 2 ₁	<i>P</i> 2 ₁ / <i>c</i>	<i>P</i> 2 ₁ / <i>c</i>
Unit cell dimensions	a = 10.0282(5) Å	a = 15.7628(5) Å	a = 10.176(2) Å
	b = 19.3323(9) Å	b = 12.1123(4) Å	b = 19.387(6) Å
	c = 19.4044(10) Å	c = 19.7909(7) Å	c = 20.093(5) Å
	α = 90°	α = 90°	α = 90°
	β = 101.790(2)°	β = 90.746(2)°	β = 102.988(9)°
	γ = 90°	γ = 90°	γ = 90°
Volume/Å ³	3682.5(3)	3776.8(2)	3862.3(17)
Z	2	4	4
Density (calculated)/g/cm ³	1.408	1.385	1.348
Absorption coefficient/mm ⁻¹	2.158	11.719	2.058
F(000)	1604.0	1612.0	1612.0
Theta range for data collection	3.006 to 55.04°	5.61 to 136.88	5.428 to 54.924
Index ranges	-13 ≤ h ≤ 13	-19 ≤ h ≤ 18	-13 ≤ h ≤ 13
	-25 ≤ k ≤ 25	-14 ≤ k ≤ 14	-25 ≤ k ≤ 25
	-25 ≤ l ≤ 25	-23 ≤ l ≤ 23	-26 ≤ l ≤ 26
Reflections collected	76565	40780	86187
Independent reflections	16866 [R _{int} = 0.0556 R _{sigma} = 0.0492]	6905 [R _{int} = 0.0470 R _{sigma} = 0.0314]	8828 [R _{int} = 0.0396 R _{sigma} = 0.0181]
Data/restraints/parameters	16866/19/793	6905/24/406	8828/0/400
Goodness-of-fit on F ²	1.036	1.025	1.078
Final R indexes [I ≥ 2σ (I)]	R ₁ = 0.0301 wR ₂ = 0.0643	R ₁ = 0.0291 wR ₂ = 0.0665	R ₁ = 0.0211 wR ₂ = 0.0443
Final R indexes [all data]	R ₁ = 0.0365 wR ₂ = 0.0666	R ₁ = 0.0394 wR ₂ = 0.0716	R ₁ = 0.0255 wR ₂ = 0.0459
Largest diff. peak/hole / e Å ⁻³	1.14/-0.61	0.73/-0.69	0.47/-0.67

Table S2 Selected Bond Lengths (Å) and Bond Angles (°) for **1-3**.

Complex 1			
Dy1-O1	2.425(4)	O1-Dy1-N4	172.00(14)
Dy1-N4	2.499(5)	O1-Dy1-C8	101.97(15)
Dy1-N1	2.249(5)	N4-Dy1-C8	70.18(15)
Dy1-C8	2.999(5)	N1-Dy1-O1	101.28(16)
Dy1-N3	2.249(4)	N1-Dy1-N4	83.95(16)
Dy1-N2	2.263(5)	N1-Dy1-C8	135.05(16)
Dy2-N8	2.527(5)	N1-Dy1-N3	117.54(17)
Dy2-O2	2.409(5)	N1-Dy1-N2	114.39(17)
Dy2-N7	2.242(5)	N3-Dy1-O1	88.72(15)
Dy2-N5	2.265(5)	N3-Dy1-N4	83.47(16)
Dy2-N6	2.247(5)	N3-Dy1-C8	26.76(16)
Si1-N1	1.719(5)	N3-Dy1-N2	124.50(17)
Si1-C30	1.865(7)	N2-Dy1-O1	99.38(16)
Si1-C29	1.860(7)	N2-Dy1-N4	83.73(16)
Si1-C31	1.888(7)	N2-Dy1-C8	99.01(16)
Si6-N7	1.719(5)	O2-Dy2-N8	171.40(16)
Si6-C67	1.855(7)	N7-Dy2-N8	82.78(16)
Si6-C66	1.861(7)	N7-Dy2-O2	102.63(16)
Si6-C68	1.887(8)	N7-Dy2-N5	115.50(17)
Si2-N2	1.720(5)	N7-Dy2-N6	116.39(17)
Si2-C33	1.890(7)	N5-Dy2-N8	83.44(18)
Si2-C34	1.875(7)	N5-Dy2-O2	99.92(18)
Si3-N3	1.714(5)	N6-Dy2-N8	82.89(17)
Si5-N6	1.723(5)	N6-Dy2-O2	88.69(16)
Si4-N5	1.707(5)	N6-Dy2-N5	123.75(18)

Complex 2			
Dy1-N3	2.253(3)	N3-Dy1-N4	83.90(9)
Dy1-N4	2.500(2)	N3-Dy1-N1	118.59(10)
Dy1-N1	2.258(3)	N3-Dy1-N5	93.77(10)
Dy1-N2	2.242(3)	N3-Dy1-C27	135.46(9)
Dy1-N5	2.532(3)	N1-Dy1-N4	85.18(9)
Si1-N1	1.715(3)	N1-Dy1-N5	100.86(10)
Si1-C29	1.875(4)	N1-Dy1-C27	26.77(9)
Si1-C30	1.862(4)	N2-Dy1-N3	117.83(9)
Si1-N2	1.718(3)	N2-Dy1-N4	83.20(9)
Si2-C9	1.868(4)	N2-Dy1-N1	120.44(10)
Si2-C8	1.870(4)	N2-Dy1-N5	92.98(10)
Si2-C10	1.867(4)	N2-Dy1-C27	95.50(9)
Si3-N3	1.717(3)	N5-Dy1-C27	114.31(10)
Si3-C18	1.870(4)	N1-Si1-C29	113.49(17)

Si3-C20	1.866(4)	N1-Si1-C28	110.85(17)
Si3-C19	1.863(4)	N1-Si1-C30	110.09(16)
N3-C13	1.412(4)	N2-Si2-C9	107.29(15)
N4-C11	1.491(4)	N2-Si2-C8	111.68(16)
N4-C21	1.491(4)	N2-Si2-C10	113.40(16)
N4-C1	1.491(4)	N3-Si3-C18	111.23(16)
N1-C27	1.419(4)	N3-Si3-C20	109.09(16)
N2-C3	1.416(4)	N3-Si3-C19	114.02(17)
N5-C31	1.326(5)	Si3-N3-Dy1	130.84(14)
N5-C35	1.287(6)	C13-N3-Dy1	109.75(19)
C1-N4-Dy1	110.61(18)	C11-N4-Dy1	109.88(17)
Si1-N1-Dy1	135.42(14)	C21-N4-Dy1	108.21(18)
C27-N1-Dy1	107.4(2)	Si2-N2-Dy1	129.61(14)
C3-N2-Dy1	111.05(19)	C31-N5-Dy1	122.5(3)
C35-N5-Dy1	121.5(3)	N1-C27-Dy1	45.79(14)
C22-C27-Dy1	94.2(2)	C26-C27-Dy1	129.3(2)

Complex 3

Dy1-O1	2.1686(14)	N1-C13	1.407(3)
Dy1-N4	2.5884(17)	O1-Dy1-N4	178.67(6)
Dy1-N3	2.2720(17)	O1-Dy1-N3	100.50(6)
Dy1-N2	2.2904(18)	O1-Dy1-N2	99.08(6)
Dy1-N1	2.2684(17)	O1-Dy1-N1	97.71(6)
Si2-N2	1.7208(18)	N3-Dy1-N4	80.82(6)
Si1-N1	1.7188(18)	N3-Dy1-N2	118.06(6)
Si3-N3	1.7150(19)	N2-Dy1-N4	80.46(6)
Si2-C9	1.875(2)	N1-Dy1-N4	81.50(6)
Si2-C8	1.879(2)	N1-Dy1-N3	113.35(6)
Si2-C7	1.881(2)	N1-Dy1-N2	121.23(6)
Si1-C6	1.869(2)	N2-Si2-C9	109.13(10)
Si1-C5	1.873(3)	N2-Si2-C8	114.95(10)
Si1-C4	1.874(3)	N2-Si2-C7	110.76(10)
Si3-C12	1.874(3)	N1-Si1-C6	110.69(10)
Si3-C11	1.875(2)	N1-Si1-C5	108.17(10)
Si3-C10	1.888(3)	N1-Si1-C4	114.65(11)
O1-N5	1.378(2)	N3-Si3-C12	109.15(10)
N4-C26	1.495(3)	N3-Si3-C11	110.78(11)
N4-C19	1.495(3)	N3-Si3-C10	113.45(11)
N4-C33	1.496(3)	N5-O1-Dy1	175.81(13)
N5-C1	1.495(3)	Si1-N1-Dy1	129.04(9)
N5-C3	1.490(3)	Si3-N3-Dy1	124.80(9)
N5-C2	1.497(3)	C33-N4-Dy1	110.98(12)
N3-C27	1.418(3)	C13-N1-Dy1	109.08(12)
N2-C20	1.414(3)	C27-N3-Dy1	114.34(13)

Table S3 Relaxation fitting parameters from least-squares fitting of $\chi(f)$ data under 500 Oe dc field of **1**.

$T(K)$	χ_T	χ_s	α
2	3.991	1.416	0.266
2.3	3.769	1.261	0.184
2.6	3.512	1.147	0.111
3	3.167	1.008	0.051
3.3	2.947	0.946	0.016
3.6	2.743	0.841	0.031
4	2.476	0.764	0.014
4.3	2.325	0.762	0.023
4.6	2.175	0.724	0.017
5	2.011	0.719	0.019
5.5	1.837	0.741	0.021
6	1.686	0.838	0.015

Table S4 Relaxation fitting parameters from least-squares fitting of $\chi(f)$ data under 500 Oe dc field of **2**.

$T(K)$	χ_T	χ_s	α
2.6	3.278	0.510	0.437
3	2.926	0.872	0.338
3.3	2.692	1.110	0.212
3.6	2.488	1.070	0.160
4	2.244	1.012	0.078
4.3	2.101	0.841	0.109
4.6	1.967	0.675	0.074
5	1.818	0.130	0.106
5.5	1.659	2.24×10^{-11}	0.145
6	1.528	3.81×10^{-11}	0.231

Table S5 Relaxation fitting parameters from least-squares fitting of $\chi(f)$ data under 500 Oe dc field of **3**.

$T(K)$	χ_T	χ_s	α
2	4.453	0.657	0.372
2.3	4.084	0.613	0.304
2.6	3.748	0.542	0.288
3	3.370	0.477	0.296
3.3	3.102	0.447	0.317
3.6	2.842	0.488	0.323
4	2.570	0.703	0.302
4.3	2.394	0.833	0.297
4.6	2.222	0.931	0.272
5	2.053	1.014	0.258
5.5	1.871	1.036	0.273
6	1.720	1.079	0.299

Table S6 Calculated energy levels (cm^{-1}), \mathbf{g} (g_x, g_y, g_z) tensors and predominant m_J values of the lowest eight Kramers doublets (KDs) of complexes **1a**, **1b**, **2** and **3**, using CASSCF/RASSI-SO with OpenMolcas.

KDs	1a			1b		
	E	\mathbf{g}	m_J	E	\mathbf{g}	m_J
0	0.0	0.180 0.437 19.284	$\pm 15/2$	0.0	0.124 0.279 19.410	$\pm 15/2$
1	140.7	10.385 8.330 2.506	$\pm 13/2$	160.7	1.945 4.763 13.550	$\pm 13/2$
2	213.2	6.646 4.333 1.681	$\pm 5/2$	246.3	7.781 5.448 2.258	$\pm 9/2$
3	295.2	1.051 3.490 12.742	$\pm 7/2$	334.2	0.263 3.509 10.837	$\pm 5/2$
4	343.2	0.118 1.868 15.017	$\pm 3/2$	378.0	0.607 1.546 17.046	$\pm 1/2$
5	368.8	1.223 1.924 16.719	$\pm 1/2$	396.3	1.595 2.182 15.897	$\pm 3/2$
6	469.3	0.250 0.336 19.110	$\pm 11/2$	534.5	0.185 0.467 18.461	$\pm 11/2$
7	574.7	0.036 0.080 19.681	$\pm 9/2$	579.6	0.166 0.610 19.073	$\pm 7/2$
KDs	2			3		
	E	\mathbf{g}	m_J	E	\mathbf{g}	m_J
0	0.0	0.902 3.871 16.514	$\pm 15/2$	0	0.0	0.127 0.316 19.054
1	71.7	3.556 5.248 7.447	$\pm 9/2$	1	83.8	0.575 1.851 14.941
2	160.4	6.167 5.012 3.482	$\pm 5/2$	2	112.2	0.530 1.007 17.069

3	260.7	1.859 4.121 11.939	$\pm 11/2$	3	161.3	3.925 5.182 11.268
4	288.1	1.513 1.899 16.835	$\pm 3/2$	4	203.0	1.533 2.297 13.292
5	393.1	0.334 1.754 17.172	$\pm 1/2$	5	261.1	0.075 2.161 14.872
6	407.8	0.511 2.421 15.505	$\pm 7/2$	6	274.6	0.529 2.279 14.878
7	419.0	0.174 1.224 17.290	$\pm 13/2$	7	403.5	0.007 0.020 19.732

Table S7 Wave functions with definite projection of the total moment $|m_J\rangle$ for the lowest eight KDs of complexes **1a**, **1b**, **2** and **3** using CASSCF/RASSI-SO with OpenMolcas.

	states	E/cm^{-1}	wave functions
1a	KD ₀	0.0	92.9% $ \pm 15/2\rangle$
	KD ₁	140.7	42.2% $ \pm 13/2\rangle$ +22.9% $ \pm 9/2\rangle$ +15.7% $ \pm 5/2\rangle$
	KD ₂	213.2	19.5% $ \pm 13/2\rangle$ +27.1% $ \pm 11/2\rangle$ +27.7% $ \pm 7/2\rangle$ +11.2% $ \pm 3/2\rangle$
	KD ₃	295.2	20.8% $ \pm 13/2\rangle$ +22.9% $ \pm 5/2\rangle$ +24.9% $ \pm 3/2\rangle$ +12.6% $ \pm 1/2\rangle$ +9.6% $ \pm 11/2\rangle$
	KD ₄	343.2	11.1% $ \pm 13/2\rangle$ +20.8% $ \pm 11/2\rangle$ +23.2% $ \pm 9/2\rangle$ +27.2% $ \pm 1/2\rangle$ +6.8% $ \pm 7/2\rangle$ +6.7% $ \pm 3/2\rangle$
	KD ₅	368.8	17.7% $ \pm 11/2\rangle$ +16.0% $ \pm 9/2\rangle$ +19.9% $ \pm 7/2\rangle$ +14.8% $ \pm 5/2\rangle$ +10.9% $ \pm 3/2\rangle$ +18.1% $ \pm 1/2\rangle$
	KD ₆	469.3	13.8% $ \pm 11/2\rangle$ +19.5% $ \pm 9/2\rangle$ +18.4% $ \pm 7/2\rangle$ +18.7% $ \pm 5/2\rangle$ +19.1% $ \pm 3/2\rangle$ +7.2% $ \pm 1/2\rangle$
	KD ₇	574.7	11.0% $ \pm 9/2\rangle$ +17.7% $ \pm 7/2\rangle$ +20.5% $ \pm 5/2\rangle$ +21.3% $ \pm 3/2\rangle$ +23.9% $ \pm 1/2\rangle$
1b	KD ₀	0.0	94.0% $ \pm 15/2\rangle$
	KD ₁	160.7	54.6% $ \pm 13/2\rangle$ +19.9% $ \pm 9/2\rangle$ +11.1% $ \pm 5/2\rangle$
	KD ₂	246.3	16.4% $ \pm 13/2\rangle$ +30.9% $ \pm 11/2\rangle$ +25.3% $ \pm 7/2\rangle$ +11.5% $ \pm 3/2\rangle$
	KD ₃	334.2	19.5% $ \pm 13/2\rangle$ +15.0% $ \pm 11/2\rangle$ +14.0% $ \pm 9/2\rangle$ +22.8% $ \pm 5/2\rangle$ +21.9% $ \pm 3/2\rangle$
	KD ₄	378.0	15.1% $ \pm 11/2\rangle$ +17.7% $ \pm 9/2\rangle$ +10.6% $ \pm 7/2\rangle$ +9.0% $ \pm 5/2\rangle$ +12.9% $ \pm 3/2\rangle$ +30.0% $ \pm 1/2\rangle$
	KD ₅	396.3	17.9% $ \pm 11/2\rangle$ +20.0% $ \pm 9/2\rangle$ +20.9% $ \pm 7/2\rangle$ +10.0% $ \pm 5/2\rangle$ +22.5% $ \pm 1/2\rangle$
	KD ₆	534.5	10.4% $ \pm 11/2\rangle$ +13.8% $ \pm 9/2\rangle$ +11.6% $ \pm 7/2\rangle$ +20.4% $ \pm 5/2\rangle$ +29.2% $ \pm 3/2\rangle$ +12.2% $ \pm 1/2\rangle$
	KD ₇	579.6	13.8% $ \pm 9/2\rangle$ +23.9% $ \pm 7/2\rangle$ +21.3% $ \pm 5/2\rangle$ +14.8% $ \pm 3/2\rangle$ +21.3% $ \pm 1/2\rangle$
2	KD ₀	0.0	70.8% $ \pm 15/2\rangle$ +12.1% $ \pm 11/2\rangle$ +9.2% $ \pm 7/2\rangle$
	KD ₁	71.7	12.2% $ \pm 15/2\rangle$ +22.6% $ \pm 13/2\rangle$ +24.4% $ \pm 9/2\rangle$ +20.9% $ \pm 5/2\rangle$ +9.4% $ \pm 1/2\rangle$
	KD ₂	160.4	13.2% $ \pm 15/2\rangle$ +20.7% $ \pm 13/2\rangle$ +17.7% $ \pm 11/2\rangle$ +23.1% $ \pm 7/2\rangle$ +13.7% $ \pm 3/2\rangle$
	KD ₃	260.7	29.1% $ \pm 13/2\rangle$ +17.1% $ \pm 11/2\rangle$ +10.3% $ \pm 9/2\rangle$ +9.3% $ \pm 7/2\rangle$ +11.0% $ \pm 5/2\rangle$ +19.9% $ \pm 1/2\rangle$
	KD ₄	288.1	21.8% $ \pm 5/2\rangle$ +29.3% $ \pm 3/2\rangle$ +22.0% $ \pm 1/2\rangle$ +9.0% $ \pm 7/2\rangle$
	KD ₅	393.1	12.2% $ \pm 9/2\rangle$ +17.1% $ \pm 7/2\rangle$ +22.1% $ \pm 5/2\rangle$ +19.5% $ \pm 3/2\rangle$ +24.2% $ \pm 1/2\rangle$

	KD ₆	407.8	17.3% ±11/2>+15.8% ±9/2>+14.8% ±5/2>+22.3% ±3/2>+16.0% ±1/2>
	KD ₇	419.0	11.9% ±13/2>+26.8% ±11/2>+24.2% ±9/2>+22.5% ±7/2>+6.9% ±5/2>
3	KD ₀	0.0	88.1% ±15/2>+8.4% ±11/2>
	KD ₁	83.8	49.7% ±13/2>+21.0% ±9/2>+8.7% ±7/2>+6.3% ±11/2>
	KD ₂	112.2	35.1% ±1/2>+29.5% ±3/2>+17.7% ±5/2>+5.8% ±13/2>
	KD ₃	161.3	12.4% ±13/2>+21.5% ±11/2>+16.5% ±7/2>+19.1% ±3/2>+16.5% ±1/2>
	KD ₄	203.0	23.2% ±7/2>+34.4% ±5/2>+12.9% ±3/2>+8.7% ±9/2>+9.2% ±13/2>
	KD ₅	261.0	12.8% ±13/2>+28.2% ±11/2>+25.2% ±9/2>+19.4% ±7/2>+8.7% ±5/2>
	KD ₆	274.7	9.6% ±13/2>+23.5% ±11/2>+32.7% ±9/2>+16.1% ±7/2>+8.2% ±5/2>
	KD ₇	403.5	11.0% ±7/2>+18.2% ±5/2>+27.7% ±3/2>+34.9% ±1/2>

Table S8 Calculated crystal-field parameters $B(k, q)$ and the corresponding weights for compounds **1a**, **1b**, **2** and **3** using CASSCF/RASSI-SO with OpenMolcas.

1a				1b			
k	q	$B(k, q)$	Weight (%)	k	q	$B(k, q)$	Weight (%)
2	-2	-0.8059×10^0	5.89	2	-2	0.3451×10^0	2.58
	-1	-0.4799×10^{-1}	0.35		-1	0.1266×10^0	0.95
	0	-0.1900×10^1	13.89		0	-0.2173×10^1	16.23
	1	0.9764×10^0	7.14		1	-0.9865×10^0	7.37
	2	0.1540×10^1	11.26		2	0.1422×10^1	10.62
4	-4	0.4223×10^{-4}	0.05	4	-4	0.6635×10^{-4}	0.08
	-3	-0.2564×10^{-3}	0.34		-3	-0.3541×10^{-3}	0.48
	-2	0.2679×10^{-2}	3.55		-2	-0.1019×10^{-2}	1.38
	-1	0.3140×10^{-3}	0.41		-1	-0.4204×10^{-3}	0.56
	0	-0.4347×10^{-2}	5.76		0	-0.4542×10^{-2}	6.15
	1	-0.4345×10^{-2}	5.76		1	0.4517×10^{-2}	6.12
	2	0.5615×10^{-2}	7.44		2	0.5926×10^{-2}	8.03
	3	-0.3294×10^{-2}	4.36		3	0.3513×10^{-2}	4.76
6	4	-0.8820×10^{-2}	11.70	4	-0.9211×10^{-2}	12.48	
	-6	0.1678×10^{-4}	2.08	6	-6	-0.9665×10^{-5}	1.22
	-5	0.3630×10^{-5}	0.45		-5	0.1843×10^{-5}	0.23
	-4	0.4637×10^{-5}	0.57		-4	-0.1155×10^{-5}	0.14
	-3	-0.1048×10^{-5}	0.13		-3	-0.1020×10^{-4}	1.29
	-2	-0.8241×10^{-5}	1.02		-2	0.4034×10^{-5}	0.51
	-1	-0.6025×10^{-5}	0.74		-1	-0.1394×10^{-4}	1.77
	0	-0.1555×10^{-4}	1.93		0	-0.1150×10^{-4}	1.46
	1	0.1437×10^{-4}	1.78		1	-0.1550×10^{-4}	1.97
	2	-0.1195×10^{-4}	1.48		2	-0.9078×10^{-5}	1.15
	3	0.1034×10^{-4}	1.28		3	-0.1115×10^{-4}	1.41
	4	-0.2470×10^{-4}	3.07		4	-0.2328×10^{-4}	2.96
5	-0.2602×10^{-4}	3.23	5		0.2755×10^{-4}	3.50	

	6	0.2290×10^{-4}	2.84		6	0.2373×10^{-4}	3.01
2				3			
<i>k</i>	<i>q</i>	<i>B</i> (<i>k</i> , <i>q</i>)	Weight (%)	<i>k</i>	<i>q</i>	<i>B</i> (<i>k</i> , <i>q</i>)	Weight (%)
2	-2	-0.1223×10^0	1.03	2	-2	0.7437×10^0	7.65
	-1	0.8921×10^{-1}	0.75		-1	0.2953×10^0	3.04
	0	-0.1188×10^1	9.96		0	-0.1055×10^1	10.86
	1	0.2054×10^0	1.72		1	0.1601×10^0	1.64
	2	0.1917×10^1	16.07		2	0.7596×10^{-1}	0.78
4	-4	-0.8416×10^{-3}	1.28	4	-4	-0.9016×10^{-3}	1.68
	-3	0.2079×10^{-3}	0.31		-3	-0.3429×10^{-3}	0.64
	-2	-0.2304×10^{-2}	3.50		-2	-0.6220×10^{-2}	11.62
	-1	-0.1594×10^{-3}	0.24		-1	-0.1420×10^{-2}	2.65
	0	-0.3845×10^{-2}	5.84		0	-0.2959×10^{-2}	5.52
	1	0.2602×10^{-2}	3.95		1	-0.5365×10^{-3}	1.00
	2	0.6851×10^{-2}	10.42		2	0.6164×10^{-2}	11.51
	3	0.4256×10^{-2}	6.47		3	-0.1279×10^{-2}	2.39
4	-0.9098×10^{-2}	13.84	4	-0.7803×10^{-2}	14.58		
6	-6	-0.6745×10^{-5}	0.96	6	-6	-0.1792×10^{-4}	3.14
	-5	-0.3191×10^{-5}	0.45		-5	-0.4628×10^{-5}	0.81
	-4	-0.1238×10^{-4}	1.76		-4	-0.1221×10^{-4}	2.13
	-3	0.3479×10^{-5}	0.49		-3	-0.1663×10^{-4}	2.91
	-2	0.1096×10^{-4}	1.56		-2	0.1842×10^{-4}	3.22
	-1	0.2523×10^{-5}	0.35		-1	-0.2215×10^{-4}	3.88
	0	-0.2138×10^{-4}	3.05		0	-0.7196×10^{-5}	1.26
	1	-0.2162×10^{-4}	3.08		1	0.5511×10^{-5}	0.96
	2	-0.6993×10^{-5}	0.99		2	0.2163×10^{-5}	0.37
	3	0.9557×10^{-6}	0.13		3	0.5988×10^{-6}	0.10
	4	-0.2889×10^{-4}	4.12		4	-0.7199×10^{-5}	1.26
	5	0.1705×10^{-4}	2.43		5	-0.4380×10^{-5}	0.76
6	0.2344×10^{-4}	3.34	6	0.1066×10^{-4}	1.86		

Table S9 Continuous Shape Measures (*CShM*) calculations for complexes **1-3**.

	Structure	PP-5	vOC-5	TBPY-5	SPY-5	JTBPY-5
1 (Dy01)	CShM	34.261	5.781	0.835	4.306	2.207
1 (Dy02)	CShM	34.407	5.892	0.890	4.412	2.185
2	CShM	35.542	7.113	0.737	5.250	1.735
3	CShM	35.217	6.537	0.531	5.027	2.512

PP-5 Pentagon (D_{5h})

vOC-5 Vacant octahedron (C_{4v})

TBPY-5 Trigonal bipyramid (D_{3h})

SPY-5 Spherical square pyramid (C_{4v})

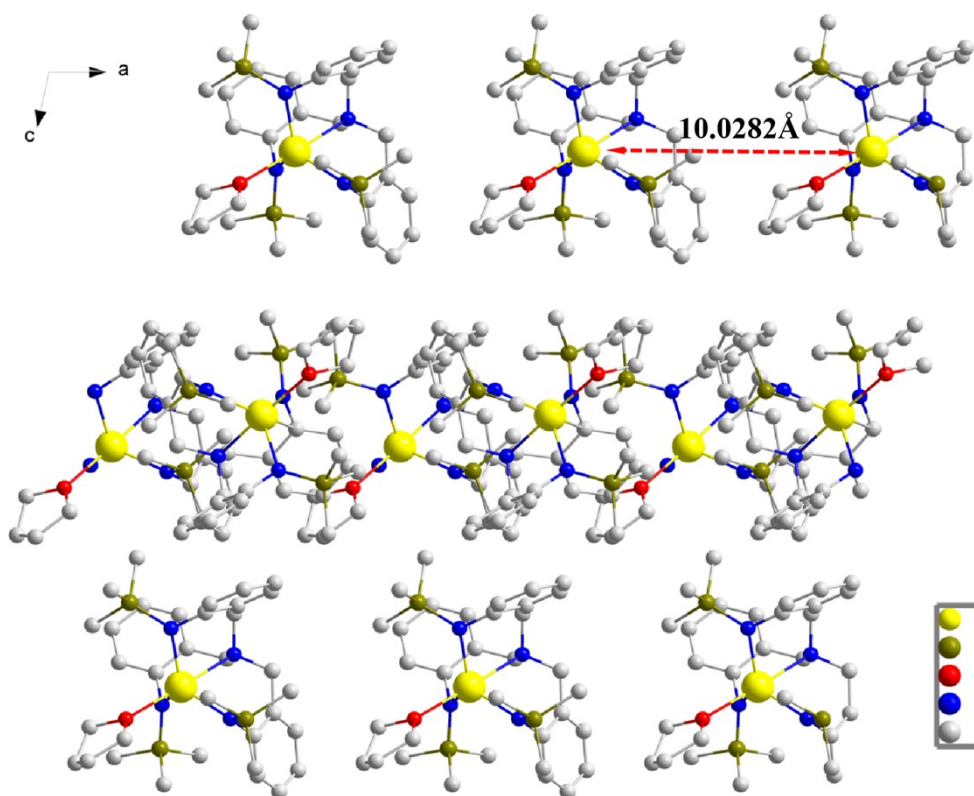
JTBPY-5 Johnson trigonal bipyramid J12 (D_{3h})

Table S10 Crystal field parameters for **1-3** fitted from magnetic data.

	B_0^2	B_0^4	B_2^4	B_0^6
1(Dy1)	301	-16	208	52
2	187	37	44	38
3	79	56	221	283

Table S11 Energy levels and g for **1-3** fitted from magnetic data.

KDs	1(Dy1)		2		3	
	E/cm^{-1}	g	E/cm^{-1}	g	E/cm^{-1}	g
1	0	0.0000	0	0.0000	0	0.0004
		0.0000		0.0000		0.0066
		19.7734		18.8536		19.0064
2	128	0.0000	91	0.0000	107	0.6460
		0.0000		0.0000		2.4864
		17.2346		15.9878		17.1728

**Fig. S1** Packing arrangement of **1** along the crystallographic b axis.

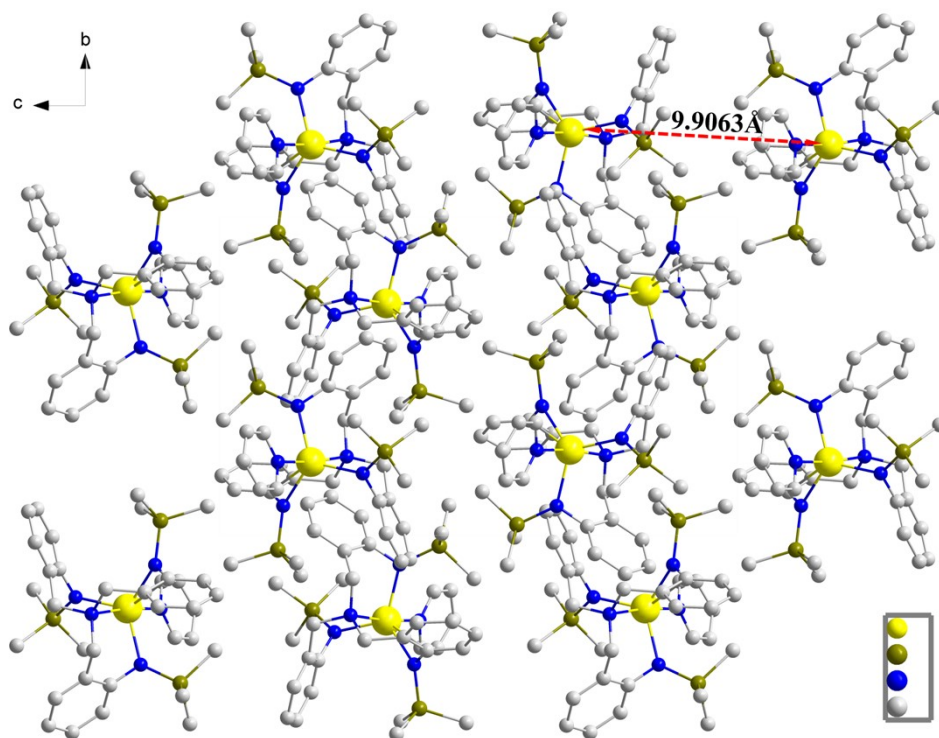


Fig. S2 Packing arrangement of **2** along the crystallographic *a* axis.

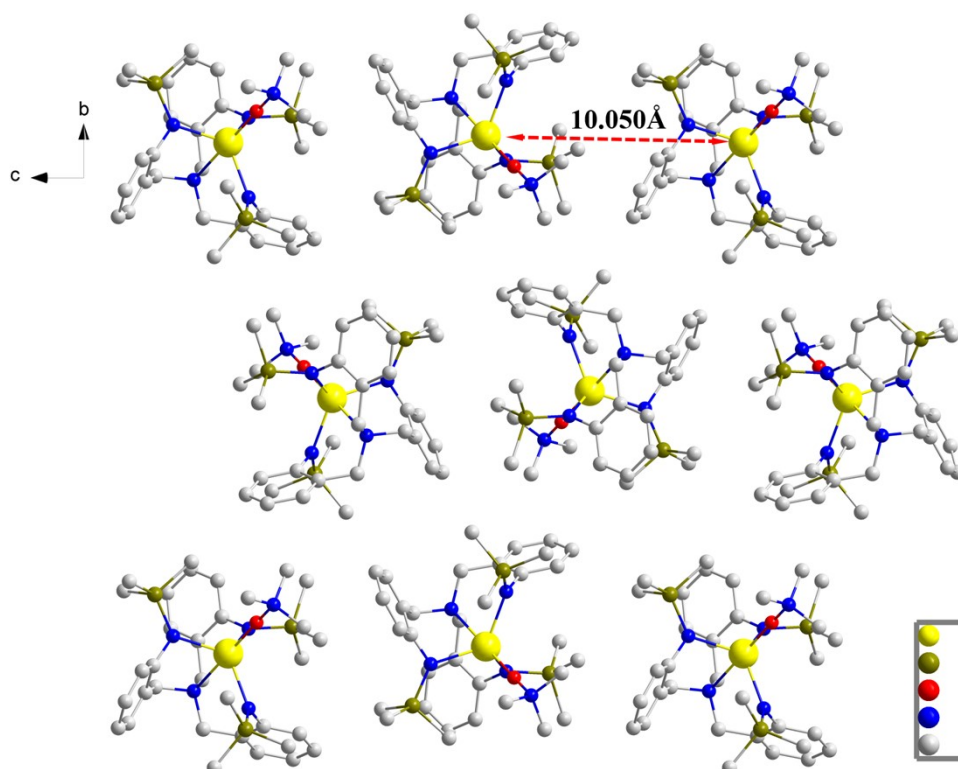


Fig. S3 Packing arrangement of **3** along the crystallographic *a* axis.

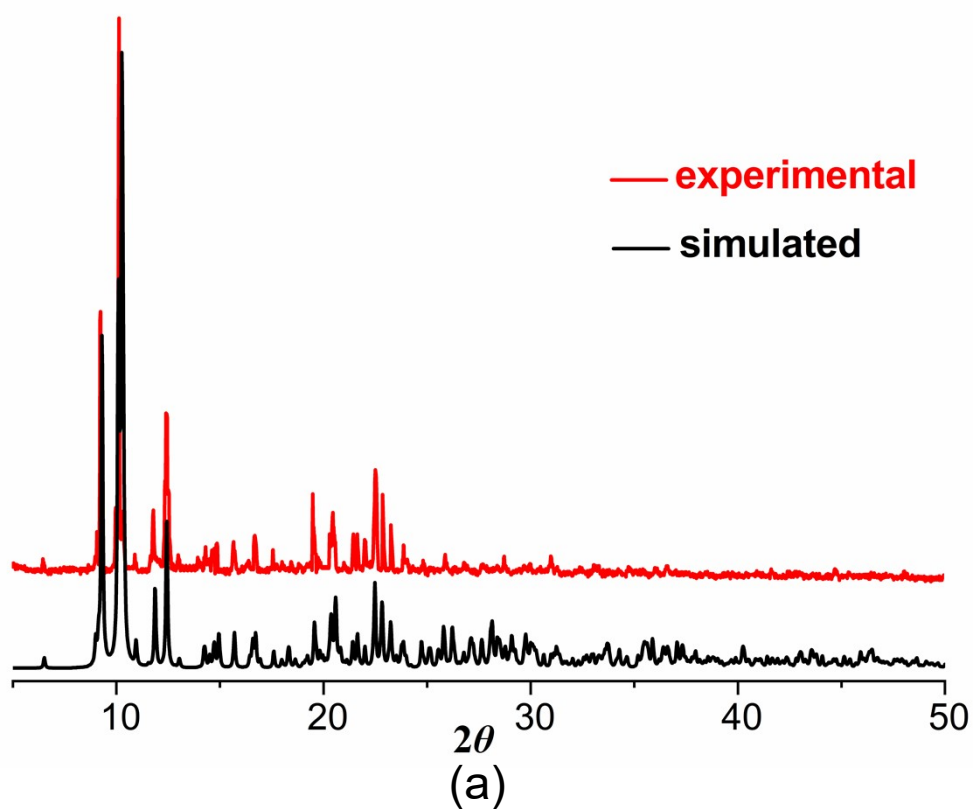


Fig. S4 PXRd patterns for complex 1.

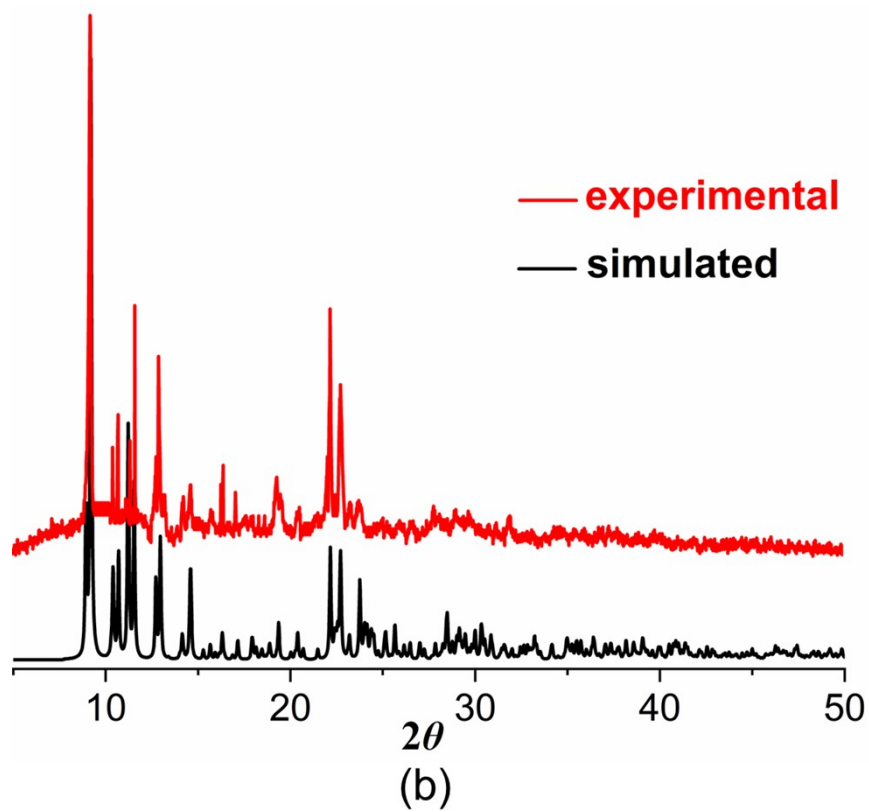


Fig. S5 PXRd patterns for complex 2.

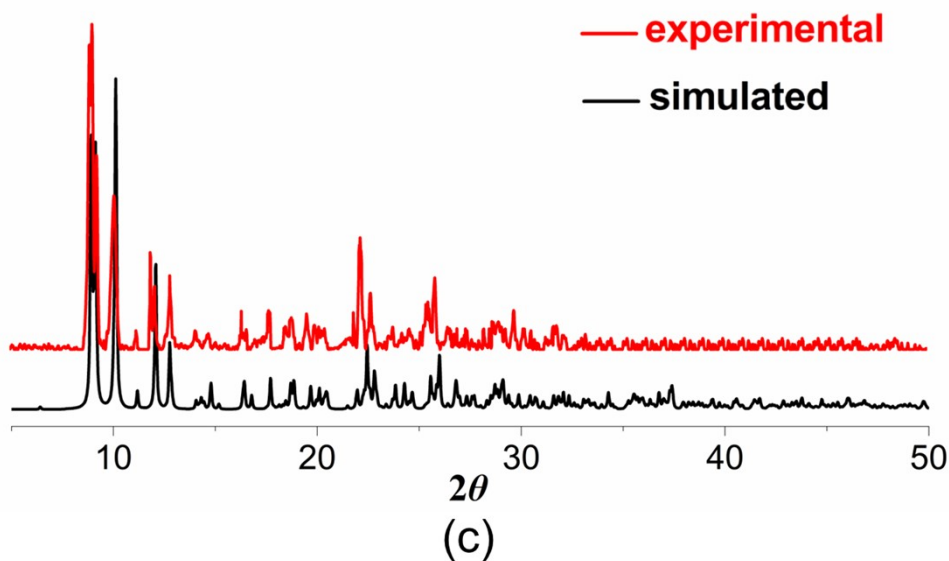


Fig. S6 PXR D patterns for complex 3.

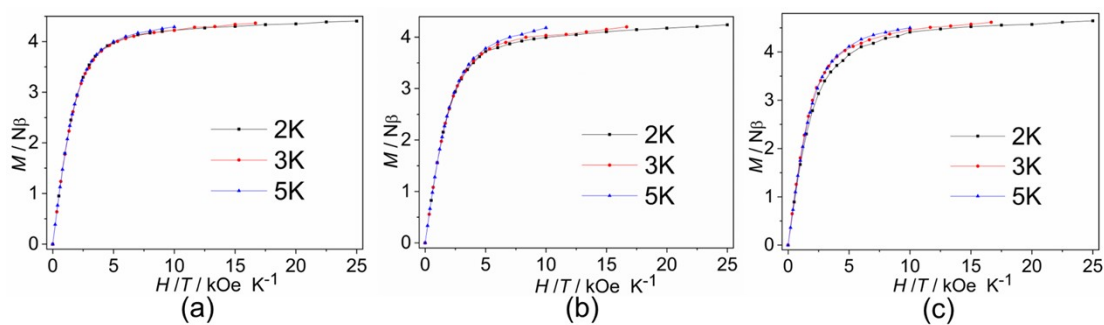


Fig. S7 Plots of M vs. H/T for 1-3 at different temperature.

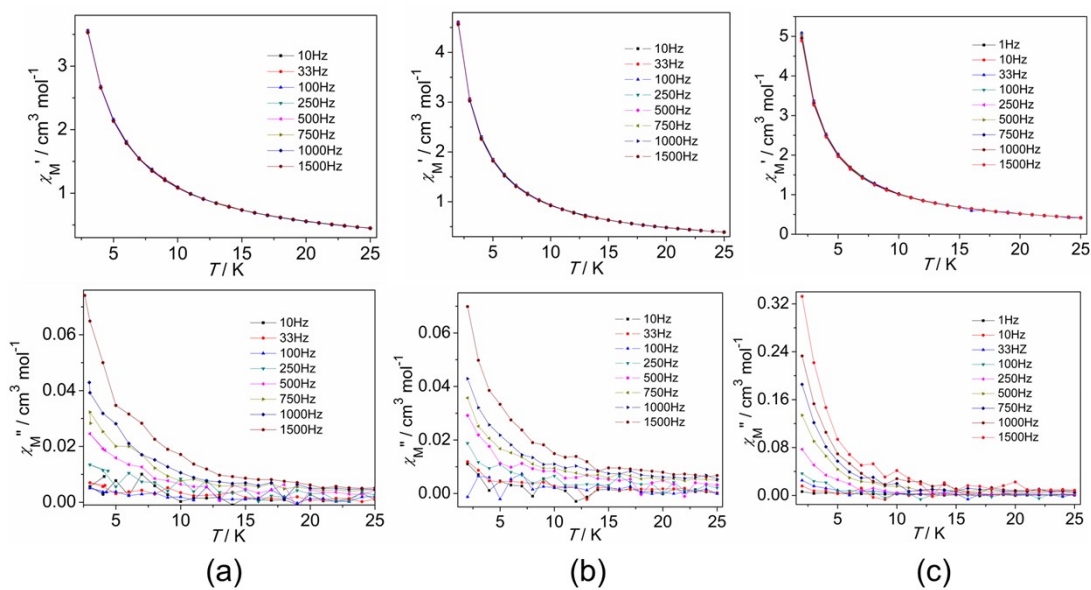


Fig. S8 Temperature dependence of the in-phase (top) and out (bottom) ac susceptibilities at different frequencies without a dc field for complexes 1-3.

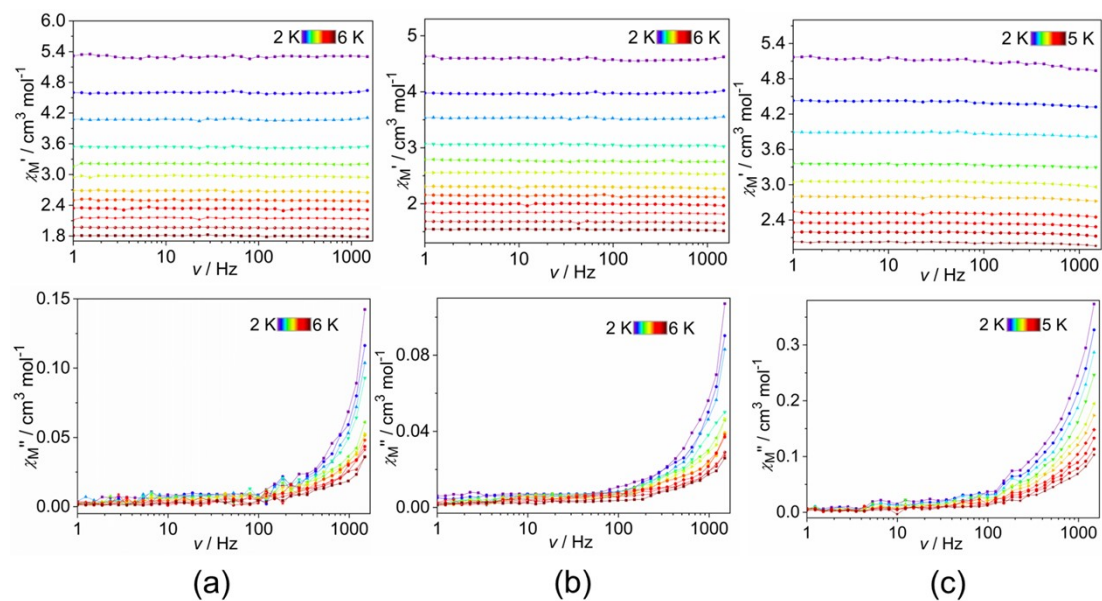


Fig. S9 Frequency dependence of the in-phase (top) and out (bottom) ac susceptibilities at different frequencies without a dc field for complexes **1-3**.

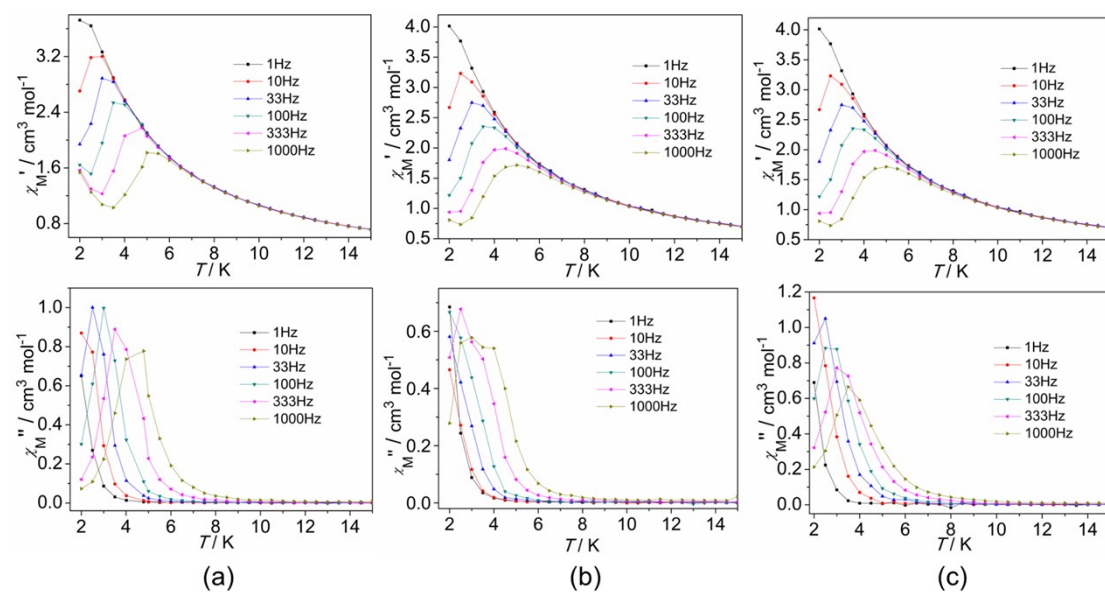


Fig. S10 Temperature dependence of the in-phase (top) and out-of-phase (bottom) ac susceptibilities at different frequencies with a dc field of 500 Oe for complexes **1** (a, a'), **2** (b, b') and **3** (c, c').

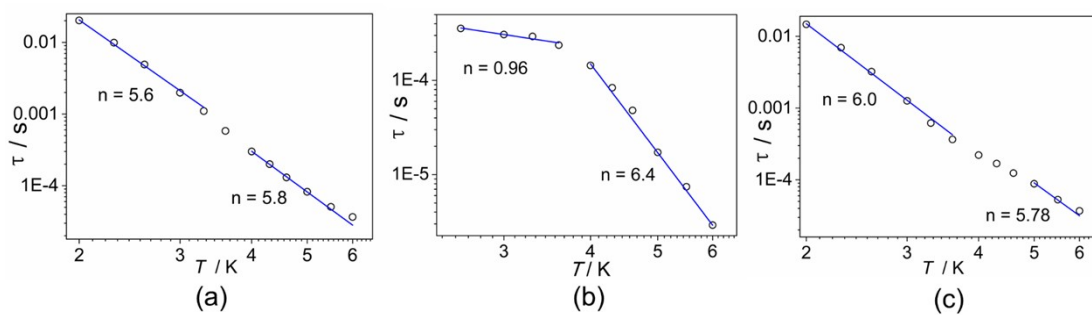


Fig. S11 Temperature dependent relaxation times of **1** (a), **2** (b) and **3** (c) (log-log scale) under a 500Oe dc field. The lines were fitted to the equation of $\tau = T^{-n}$ to give n values.

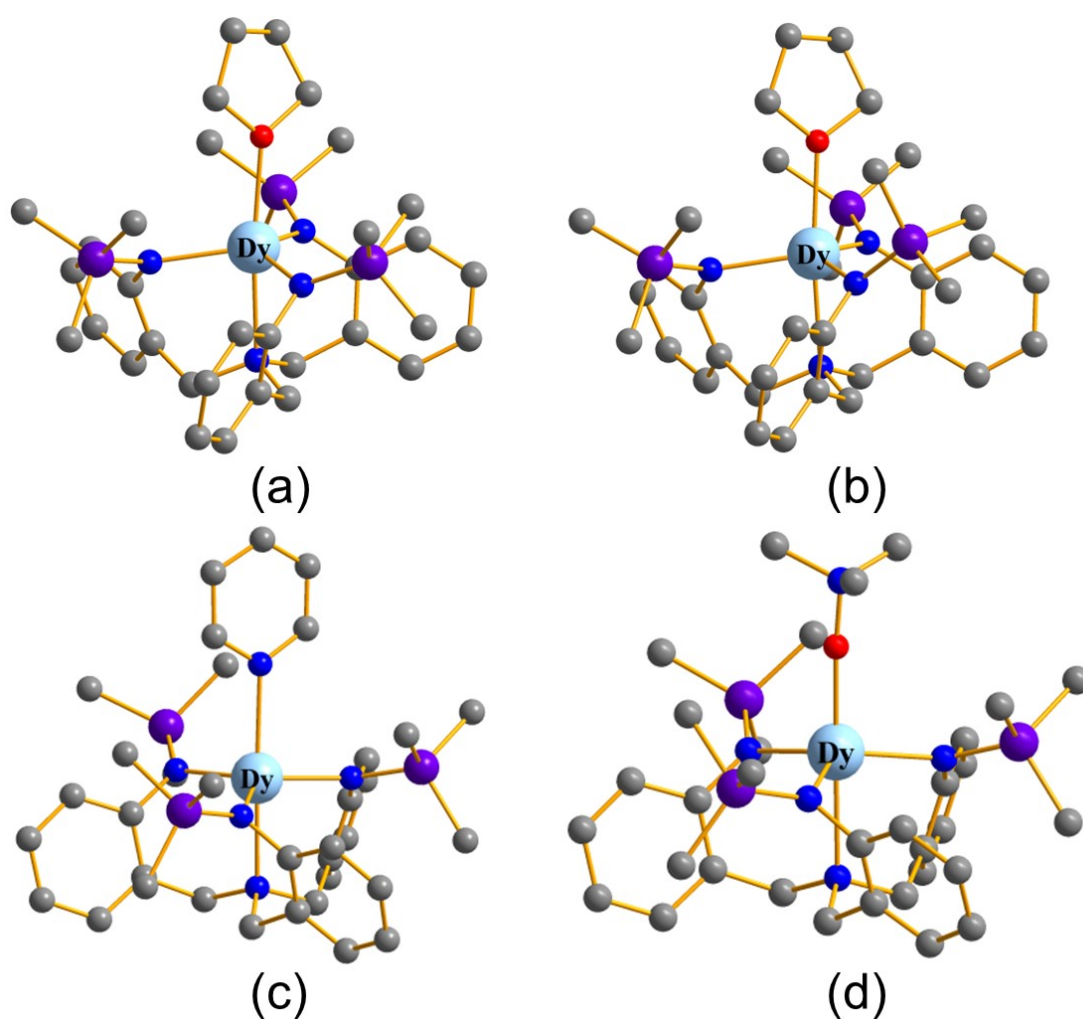


Fig. S12 Calculated molecular structures of complexes **1a** (a), **1b** (b), **2** (c) and **3** (d); H atoms are omitted for clarify.

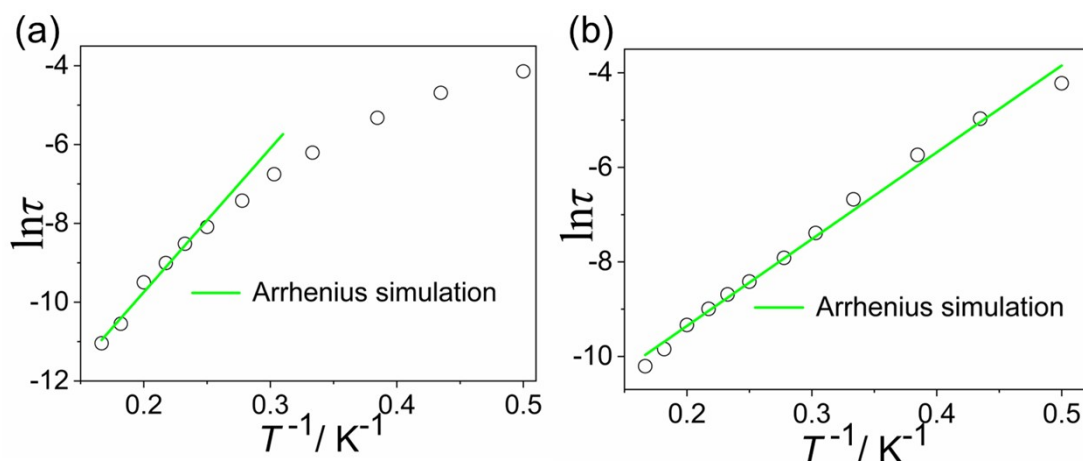


Fig. S13 Magnetization relaxation time, $\ln \tau$ vs. T^{-1} plot under 500 Oe dc field for **1** (a), **3** (b). The green line represents the Arrhenius fit.

References

- S1 Galván, I. F.; Vacher, M.; Alavi, A.; Angeli, C.; Aquilante, F.; Autschbach, J.; Bao, J. J.; Bokarev, S. I.; Bogdanov, N. A.; Carlson, R. K.; Chibotaru, L. F.; Creutzberg, J.; Dattani, N.; Delcey, M. G.; Dong, S. S.; Dreuw, A.; Freitag, L.; Frutos, L. M.; Gagliardi, L.; Gendron, F.; Giussani, A.; González, L.; Grell, G.; Guo, M. Y.; Hoyer, C. E.; Johansson, M.; Keller, S.; Knecht, S.; Kovacevic, G.; Källman, E.; Manni, G. L.; Lundberg, M.; Ma, Y. J.; Mai, S.; Malhado, J. P.; Malmqvist, P. Å.; Marquetand, P.; Mewes, S. A.; Norell, J.; Olivucci, M.; Oppel, M.; Phung, Q. M.; Pierloot, K.; Plasser, F.; Reiher, M.; Sand, A. M.; Schapiro, I.; Sharma, P.; Stein, C. J.; Sørensen, L. K.; Truhlar, D. G.; Ugandi, M.; Ungur, L.; Valentini, A.; Vancoillie, S.; Veryazov, V.; Weser, O.; Woźniowski, T. A.; Widmark, Per-Olof.; Wouters, S.; Zech, A.; Zobel, J. P.; Lindh, R. *J. Chem. Theory Comput.* **2019**, *15*, 5925-5964.
- S2 Malmqvist, P. Å.; Roos, B. O.; Schimmelpfennig, B. *Chem. Phys. Lett.* **2002**, *357*, 230-240.
- S3 Heß, B. A.; Marian, C. M.; Wahlgren, U.; Gropen, O. *Chem. Phys. Lett.* **1996**, *251*, 365-371.
- S4 Chibotaru, L. F.; Ungur, L.; Soncini, A. *Angew. Chem., Int. Ed.* **2008**, *47*, 4126-4129.
- S5 Ungur, L.; Van den Heuvel, W.; Chibotaru, L. F. *New J. Chem.* **2009**, *33*, 1224-1230.
- S6 Chibotaru, L. F.; Ungur, L.; Aronica, C.; Elmoll, H.; Pilet, G.; Luneau, D. *J. Am. Chem. Soc.* **2008**, *130*, 12445-12455.